

## Chapter 1: Introduction

### 1.1 - Thermoelectric Motivation and Applications

In a world where renewable energy is becoming an increasingly hot topic, new and different strategies have been investigated for producing it. In addition to approaches such as wind and solar power, several other approaches that focus primarily on increasing energy utilization efficiency or recovering waste heat are also being pursued. Thermoelectric materials have received a considerable amount of attention in terms of waste-heat recovery for a wide range of applications including automobiles (General Motors [1] and BMW [2]), ships and boats [3, 4], industrial processes [5], remote sensing (oil and gas [6], nuclear [7]), thermonuclear power for space missions [8, 9], or as cathodic protection devices to reduce corrosion in oil and gas pipelines [10]. Another useful application of thermoelectric materials is for solid-state refrigeration, which is useful for applications where vibrations involved with conventional refrigeration techniques are detrimental (medicinal storage, wine refrigerators, etc.) or where precisely controlled spot-cooling (or heating) is desired. Because of the broad range of potential applications and wide academic and scientific impact (in a range of fields including: thermal/electronic transport processes, metallurgical techniques, solid-state chemistry, and others), thermoelectric materials have received a significant amount of interest over the last 50-60 years.

The fundamental process responsible for thermoelectric power generation (or efficiency) is known as the Seebeck effect. Metals or doped semiconductors contain free charge carriers and produce the Seebeck effect in the presence of a temperature gradient. If we consider these carriers as a gas of charged particles, the gas will be most dense at the cold side of the material (Figure 1-1). At equilibrium, an electric field (voltage) will be generated to balance the chemical, diffusive driving force provided by the temperature difference. The Seebeck coefficient can be

written as the ratio of the measured voltage across the sample to the temperature difference,  $S \approx -\frac{\Delta V}{\Delta T}$ . The Seebeck effect is also often used in thermocouples for precise temperature measurements. While Figure 1-1 shows the effect for a single material, two unlike-materials (for example, chromel and alumel in a K-type thermocouple) coupled together will produce a voltage that depends very precisely on the temperature at their union. However, unlike precise thermocouple measurement instrumentation where the value of the Seebeck does not need to be particularly large, thermoelectric devices for waste heat recovery applications prefer a specific combination of material parameters (including large Seebeck coefficient).

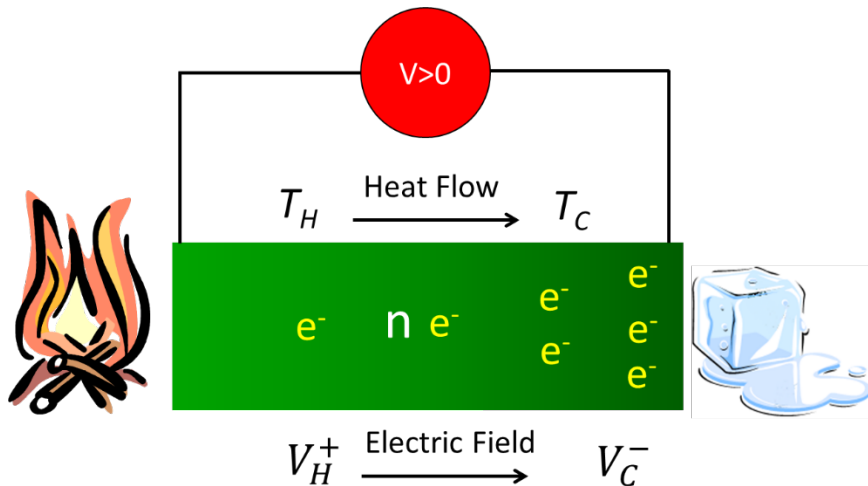


Figure 1-1: Schematic diagram of the Seebeck effect in which charge carriers diffuse towards the cold end of a heated material—the resulting voltage that develops determines the Seebeck coefficient:  $S = -\frac{\Delta V}{\Delta T}$ .

Thermoelectric efficiency is determined by the thermoelectric figure of merit:  $zT = \frac{S^2 \sigma}{\kappa} T$ , where  $S$  is the Seebeck coefficient,  $\sigma$  is the electrical conductivity,  $\kappa$  is the thermal conductivity, and  $T$  is the temperature of operation. This relation is derived by considering all of the modes of heat and current transfer through a theoretical device. Of course, a high Seebeck coefficient is preferred since this directly leads to a higher voltage across the device; good electrical conductivity is desired in order to minimize resistive losses due to Joule heating (which generates heat, reducing the overall  $\Delta T$  across the device), and a low thermal conductivity is necessary to

allow the largest possible temperature gradient. Current state-of-the-art thermoelectric materials that are used for waste heat recovery have  $zT$  values near 1.0, which corresponds to less than 12% energy conversion efficiency (for high temperature power generation) once devices losses are taken into account [6]. An average  $zT$  of 1.25 would enable substantial waste-heat harvesting and up to a 10% fuel reduction in the case of automotive applications [6]. Since the early 1990s, a wave of new nanotechnology related research has ushered in a new era for thermoelectric materials as well [11]; nanoscale features had been theorized to provide revolutionary advances beyond conventional bulk solids by either lowering thermal conductivity through modes of additional phonon-scattering or by altering the electronic structure which is known to benefit from low-dimensional features [11]. While nanoscale features have led to advances in some areas [12-14], the renewed interest in thermoelectric materials has also revitalized research efforts towards developing advanced bulk materials through conventional solid-state chemistry and physics techniques. This thesis will highlight several examples where traditional semiconductor physics including optical, electronic, and *ab-initio* computed properties are utilized in common thermoelectric materials to guide new strategies for enhancing  $zT$  using “Band Engineering.”

## 1.2 - Thermoelectric Materials, Band Engineering, and Summary of Work

Even though the scientific community’s renewed interest in thermoelectrics may have been sparked by the promise of benefits due to nanoscale features, a large number of recent advanced material discoveries involve bulk materials and alloys which owe their extraordinary performance to superior electronic properties. These discoveries can be explained in the context of semiconductor transport physics and doping without nanoscale features. The “Band Engineering” concept uses a variety of strategies for optimizing  $zT$  including either carrier concentration tuning or altering the electronic structure using alloying in order to utilize additional electronic states through band convergence. Here, I will apply band engineering techniques to resolve discrepancies observed in the literature regarding the electronic band structure

parameters (band gap, secondary band offset, effective masses, etc.) in a variety of thermoelectric materials, including IV-VI materials and their alloys (Chapter 3 and 4), ZrNiSn half Heusler's (Chapter 5), and  $\text{CoSb}_3$  skutterudite and  $\text{A}_5\text{M}_2\text{Sb}_6$  Zintl materials (Chapter 6). This is accomplished with a combination of optical absorption measurements (absorption edge), electronic/thermal/thermoelectric transport properties measurement (and corresponding semi-empirical modelling), and *ab-initio* electronic band structure calculations (traditional density functional theory, DFT, *ab-initio* molecular dynamics, AIMD, and numerical solutions to the Boltzmann transport equation, Boltztrap). Furthermore, in the context of band engineering, I develop theoretical techniques to provide a framework for analyzing DFT-computed thermoelectric transport properties (Chapter 7). Work in this thesis provides insight into the electronic band structure contributions to the thermoelectric properties for a few systems of materials of great interest to the thermoelectrics community, namely IV-VI materials, half-Heuslers, and skutterudites.

Until recently, PbTe and the IV-VI materials were thought to have a mediocre peak  $zT$  with values lower than 1.0; however, in the last five years many works have shown some of the highest recorded  $zT$  values in its alloys, approaching and exceeding 2.0 [14-21]. These recent advancements are attributed both to improvement in high temperature thermal conductivity measurements (through development of the new standard for these measurements: the laser flash technique discussed in Chapter 2) and electronic band structure engineering by doping and alloying these materials with other elements. This wave of new work on the IV-VI materials has spurred additional discussion of their band structures (particularly as a function of temperature); Chapter 4 provides a series of optical measurements, electronic properties measurements, and AIMD calculations which provide new insight into the temperature at which the primary and secondary valence bands converge (which is commonly cited as the reason for the superior performance of PbTe and its alloys).

Another family of materials, the half Heusler's with the general formula XYZ, where X=Zr, Ti, Hf, ..., Y=Ni, Co, ..., and Z=Sn, Sb, ..., have also been shown to be good thermoelectric materials. Half Heuslers are often favored over other materials because of their ability to attain high  $zT$  ( $\sim 1.0$ ) without toxic or rare elements [22, 23]. In Chapter 5 of this thesis, I use experimentally measured optical and electronic properties in ZrNiSn to determine both the value of the band gap ( $E_g \approx 0.13$  eV) and the electron-to-hole weighted mobility ratio ( $A \approx 5$ ). The low hole mobility agrees with some recent observations that the valence band may be composed of in-gap states resulting from interstitial Ni atoms, which is not captured in conventional DFT calculations. Further,  $A=5$  helps to explain the good performance of n-type ZrNiSn at high temperatures despite its narrow band gap. I also develop theory which relates the maximum in the temperature-dependent thermopower to the band gap for low gap materials with electron-to-hole weighted mobility ratios not equal to 1.0.

Another popular bulk material is CoSb<sub>3</sub>, which has proven itself a leader in commercial applications for waste heat recovery. By filling voids in the crystal structure with dopant atoms (Yb, La, In, etc.), simultaneous doping and phonon scattering (sometimes attributed to rattling of the filler atoms) leads to high  $zTs$  greater than 1.0 around 400°C. Chapter 6 of this thesis thoroughly investigates this material as a multiple-band electronic conductor. Using electronic transport measurements in a doping study, I show that the thermoelectric properties are not explainable using single band properties (even if that band is a non-parabolic Kane-type band). This is supported by the observation of multiple absorption edges observed in optical measurements. The thermoelectrics community generally attributes high  $zT$  in these materials to the reduction in thermal conductivity; however, results from this thesis indicate that it also has a superb (and possibly engineerable) electronic structure that is at least partially responsible for its high  $zT$ .

These thermoelectric material systems are quite important to the thermoelectric community. By characterizing their electronic structure, we can pave the way for band engineering and further improvement of their properties. The remainder of this introductory chapter will detail some of the fundamental concepts that link electronic and thermoelectric transport properties to a material's underlying electronic structure.

### 1.3 - Doping and $zT$ Optimization

Extrinsic doping involves the substitution of impurity atoms, which contain a different charge state than the native lattice. In order to maintain charge neutrality, additional holes or electrons are added, creating a p-type or n-type material, respectively. In thermoelectric materials, doping can lead to drastic changes in the properties and is therefore critical for optimizing  $zT$ . Figure 1-2 shows the dependence of  $zT$  and the other thermoelectric parameters on carrier concentration by assuming a single parabolic band and acoustic phonon scattering [24]. As the carrier concentration is lowered, say in the case of an insulator, the Seebeck coefficient becomes quite high, but the electrical conductivity is lowered significantly, resulting in poor  $zT$ . For high carrier concentration (as in a metal), the electrical conductivity is high, but the Seebeck is lower. For this reason,  $zT$  and power factor ( $S^2\sigma$ ) are usually optimized in the  $10^{19}$ - $10^{20}$   $\text{cm}^{-3}$  range (usually described as a heavily doped semiconductor). In the absence of extrinsic doping, the doping level for a given material is set by its intrinsic defect level, which can depend upon sample preparation procedures (annealing temperature, quench vs. slow cool) and can be quite sensitive to sample stoichiometry and defect formation energetics. Doping (intrinsic or extrinsic) often serves as a good first check to determine whether a given material's properties can be further optimized.

Using the single parabolic band (SPB) model [24] (Figure 1-2), it is straightforward to obtain information like the effective mass ( $m^*$ ), deformation potential ( $E_{def}$ , which determines the strength of electron scattering by acoustic phonons), and lattice thermal conductivity ( $\kappa_L$ ); the

combination of these parameters can be used to determine the maximum attainable  $zT$  (and the carrier concentration at which it occurs). The SPB model is a useful tool because it is easily generated from a small amount of experimental data, and it can be extremely useful when determining a  $zT$  optimization strategy for a new material.

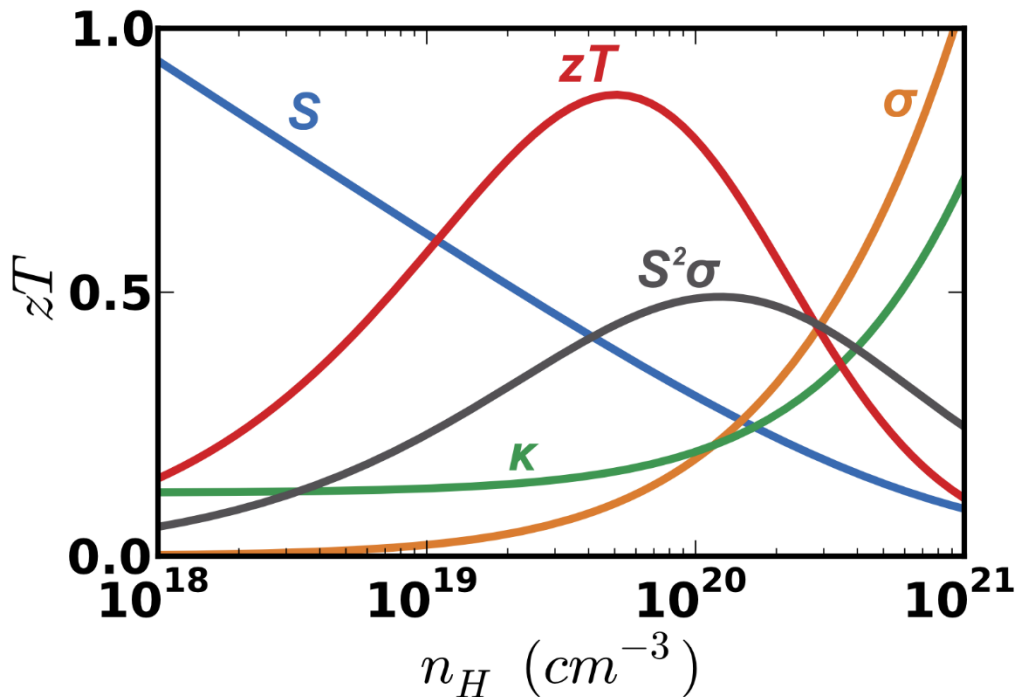


Figure 1-2: Carrier concentration dependence of  $zT$  and other thermoelectric properties.

#### 1.4 - Multiple Band Phenomena in Thermoelectric Materials

While the single parabolic band works well for a variety of systems, many of the best thermoelectric materials contain multiple electronic bands. Multi-valence band phenomena are believed to be responsible for the superior  $zTs$  in several systems, including PbTe [15-18], PbSe [25], Mg<sub>2</sub>Si [26], and others. Each band can be treated as a parallel circuit; their electrical conductivities add, but each band maintains its own high Seebeck coefficient. This leads to a greatly enhanced performance, particularly when multiple bands are occupied and at similar energy levels (converged bands lead to the largest enhancements). One of the most successful examples where converging electronic bands are beneficial to thermoelectric performance is in

PbTe. PbTe has two valence bands offset by  $\sim 0.15$  eV ( $\Delta E$ ) at 300 K as shown in Figure 1-3. The band positions are thought to change as a function of temperature, resulting in band convergence at around 400 K according to Tauber et al. [27] However, work shown in this thesis disagrees with this finding, showing an optical band gap that continues to increase with temperature until the highest measured temperature of 673K, which is supported by AIMD calculations. Alloying has also been shown to improve the thermoelectric properties for lead chalcogenide materials; the improvement is usually attributed to both reduction in the lattice thermal conductivity due to point defect scattering of phonons and an  $L - \Sigma$  band offset ( $\Delta E$ ) reduction (in the case of alkaline earth alloying on the lead site). I show one case in particular where significantly improved properties are attained using alloys of the lead-chalcogenide materials (PbSe/SrSe- Chapter 4.3,  $zT_{max} \approx 1.5$ ). This thesis includes several other examples of multiple band behavior.

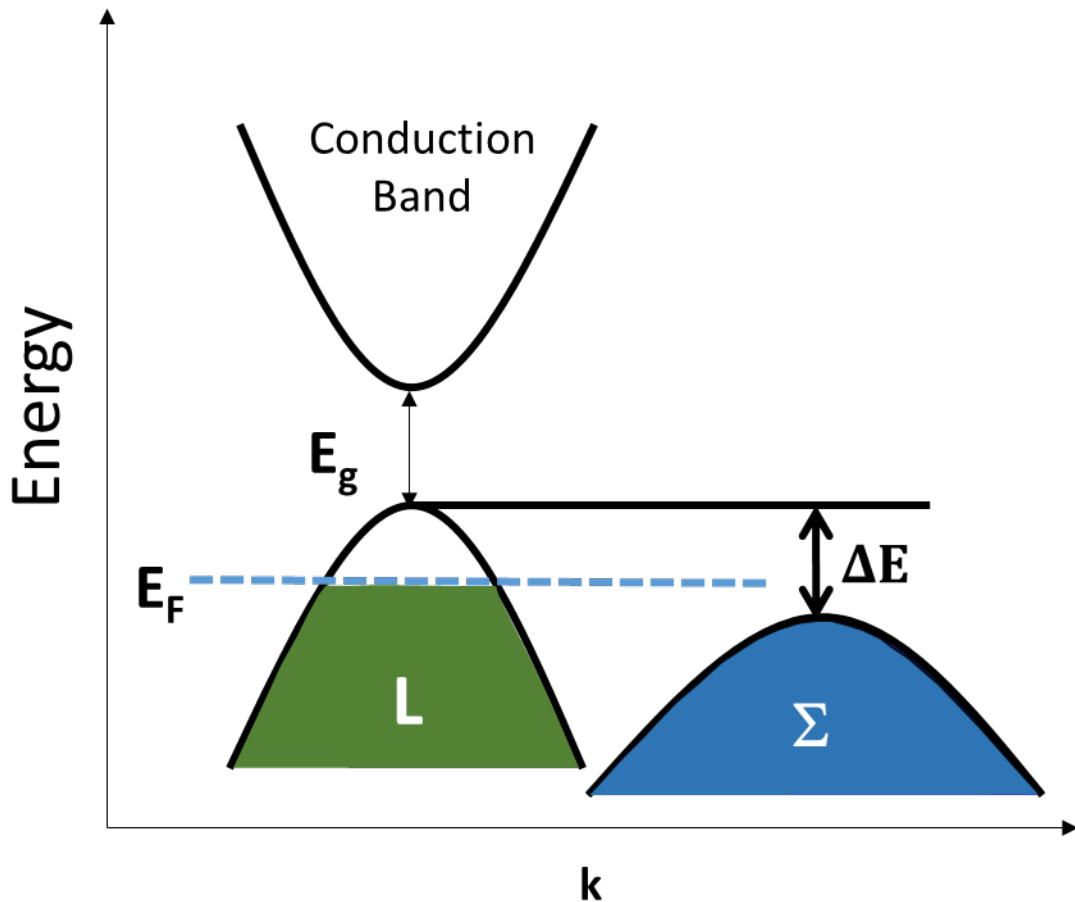


Figure 1-3: Near-edge band structure in the lead chalcogenides indicating multi-band behavior for p-type.

Besides the lead chalcogenides, Chapter 6 includes optical, electronic, and *ab-initio* calculation evidence of multi band behavior in the conduction band of  $\text{CoSb}_3$ . High temperature electronic and optical properties show band convergence, which is likely extraordinary thermoelectric performance in Yb filled  $\text{CoSb}_3$ . Otherwise, multi-band behavior is also evident in the optical and transport properties of two other systems: the 5-2-6 family of Zintl compounds,  $\text{Ca}_5\text{In}_2\text{Sb}_6$  (Chapter 6.3), and in  $\text{SnTe}$  (Chapter 4.4). By understanding the nature of the band structure, we open the door for future band engineering studies through isoelectronic alloying of these systems, which can lead to large  $zT$  enhancements.

## 1.5 - Band Gap in Thermoelectric Materials

Because many thermoelectric materials are narrow gap semiconductors ( $E_g < 0.5$  eV), their high temperature properties are often subject to strong bipolar effects. Bipolar effects occur in doped semiconductors when minority carrier states become populated and their conductivities become comparable in magnitude to the majority carrier. Because these carriers have opposite signs, the temperature dependent thermopower (defined as the magnitude of the Seebeck coefficient,  $|S|$ ) increases to a maximum and then decreases (Figure 1-4a). This is accompanied by an increase in electrical conductivity (and the electronic contribution to the total thermal conductivity,  $\kappa_{total}$ , Figure 1-4b) due to the presence of both electrons and holes. The Goldsmid-Sharp band gap allows us to relate the maximum in the temperature dependent thermopower to the band gap of a semiconductor:  $E_g = 2e|S|_{max}T_{max}$ . In terms of thermoelectric performance, this maximum in the thermopower often leads to a corresponding maximum in the  $zT$ . Because the peak  $zT$  is the metric by which most thermoelectric materials are compared, understanding the value of the band gap and the onset of bipolar conduction is critical for optimizing the temperature dependent  $zT$ .

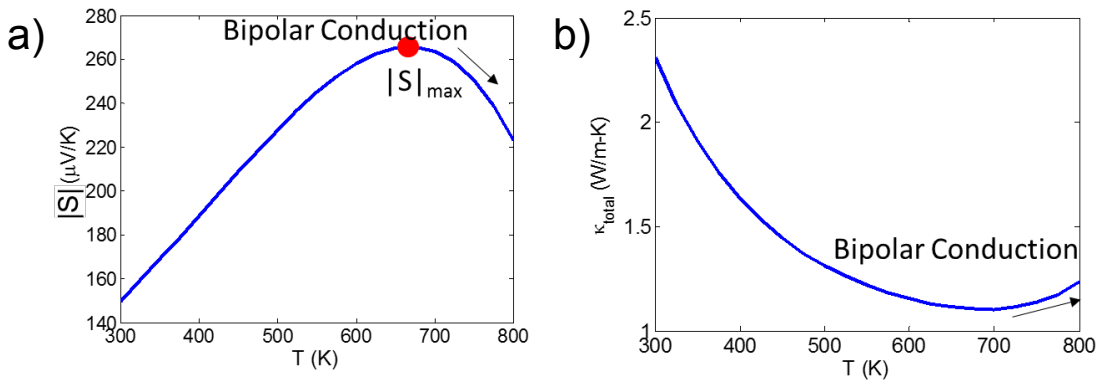


Figure 1-4: Bipolar conduction example in I-doped PbTe including a) Temperature dependent Seebeck coefficient and b) temperature dependent thermal conductivity [28].

Besides the Goldsmid-Sharp band gap, the temperature dependent resistivity can also be used to estimate the band gap for semiconductors in the intrinsic region of conductivity (low

doping levels). The electrical resistivity is related to the temperature following  $\sigma(T) = \sigma_0 \exp(-\frac{E_g}{2k_B T})$  where  $\sigma_0$  is related to both the density of states and mobility for the material.

Other than transport measurements, optical measurements such as absorption edge, photoconductivity, and photoluminescence are the most direct methods of obtaining an estimate of the band gap. In optical absorption edge measurements, a sample is illuminated by light of different frequencies (which correspond to a photon energy:  $E = \hbar\omega$ ) that can be absorbed by electrons in the valence band (Figure 1-5a). If  $\hbar\omega$  is less than the band gap energy, no absorption is observed because there are no states within the band gap to excite the valence band electrons into. However, for photon energies equal to or larger than the band gap, we observe a rapid rise in the absorption coefficient (Figure 1-5b).

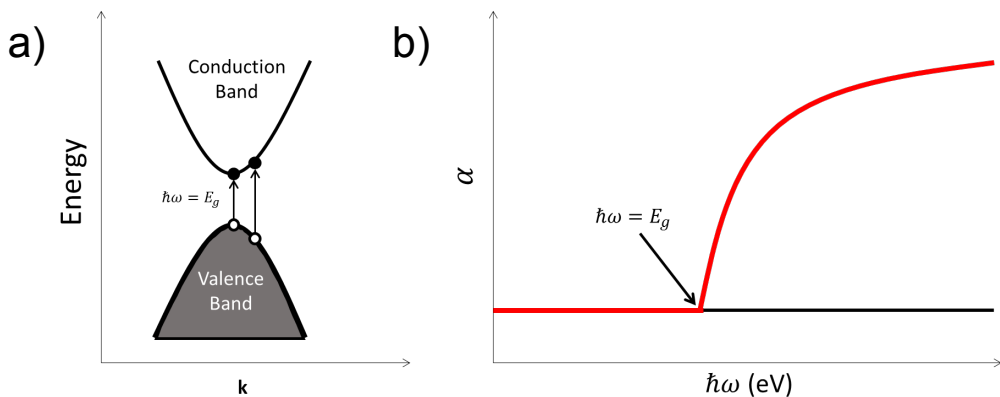


Figure 1-5: Optical absorption edge illustrating the illumination of the valence band by a photon with energy ( $\hbar\omega$ ), which excited an electron to the conduction band if  $\hbar\omega \geq E_g$ .

Experimentally, the energy at which the absorption coefficient,  $\alpha$ , begins to rise indicates the band gap energy. Usually, band gap obtained from optical measurements is understood to be more accurate (and more direct) than those obtained through electronic measurements, especially if  $E_g$  is temperature dependent. Chapter 3 of this thesis shows how sensitive optical measurements can be by investigating slight shifts in the optical absorption edge with small changes in doping level, known as the Burstein-Moss shift.

Because band gap is such an important parameter in thermoelectric materials, both in terms of bipolar conduction and band engineering strategies, estimates of the band gap are useful regardless of whether they come from electronic or optical results. Sources of discrepancies for the Goldsmid-Sharp (maximum thermopower) band gap are described in detail in Chapter 5. I show that the largest discrepancies in the computed value occurs for large electron-to-hole weighted mobility ratio ( $A$ ) and narrow band gaps. In this thesis, a large difference in the Goldsmid-Sharp band gap for p-type and n-type ZrNiSn Half-Heusler thermoelectric materials is explained by invoking a weighted mobility ratio ( $A$ ) of 5.0 (rather than 1.0, which is assumed in the derivation of Goldsmid-Sharp's  $E_g = 2eS_{max}T_{max}$  formula). The theory is developed to extend this analysis to any general  $A$ -value or measured band gap using full Fermi statistics (which are useful for thermoelectric materials which contain narrow gaps).

## 1.6 - Band Engineering from *Ab-Initio* Calculations

*Ab-initio* calculations are a useful tool for mapping the electronic structure for a material. Because this thesis focuses on connecting measured electronic, thermoelectric, and optical properties to the electronic band structure, *ab-initio* electronic band structure calculations are a crucial tool for helping to explain the results. For example, Chapter 4 shows results regarding the temperature-dependent band gap in PbTe computed using AIMD calculations that mimic the effect of atomic vibrations (phonons) on the computed electronic band structure; coupled with thermal expansion of the lattice, we correlate these calculations to the measured optical results. In another example of *ab-initio* calculations, Chapter 6 shows an electronic band structure calculation and Fermi surface mapping for CoSb<sub>3</sub>, which provide the insight needed to explain the two observed absorption edges that were measured optically. Another natural extension of *ab-initio* electronic structure calculations is to directly predict thermoelectric properties by solving the Boltzmann transport equation.

Boltztrap is a useful, open-source code that uses calculated band structures to generate Fermi-level dependent thermoelectric transport data which can be used to discover new compounds in a high-throughput sense [29, 30]. In Chapter 7 of this thesis I discuss the application of many of the band engineering strategies to Boltztrap calculations from the Material Project (materialsproject.org). I define a new, easily computed parameter known as the “Fermi surface complexity factor”,  $(N_v^*K^*)$  which is composed of both the effective valley degeneracy ( $N_v^*$ ) and the effective anisotropy factor ( $K^*$ ).  $N_v^*$  reflects the influences of multiple bands when they are near the Fermi level, while  $K^*$  is enhanced for complex Fermi surfaces (as observed in the valence bands of the III-V and IV-VI semiconductors). Further  $(N_v^*K^*)$  improves upon existing Boltztrap results by bypassing the constant relaxation time approximation (CRTA) to provide a parameter (unlike Seebeck coefficient or power factor) that reflects the electronic structure directly, is proportional to the maximum attainable power factor, and does not depend on the observed scattering mechanism.

## 1.7 - Conclusions

In this thesis, I will focus on explaining the electronic band structure origin of the thermoelectric properties in the context of band engineering for three heavily studied groups of thermoelectric materials: IV-VI semiconductors (PbTe, PbSe, PbS, SnTe), ZrNiSn half Heuslers, and  $\text{CoSb}_3$  skutterudites. I have utilized a variety of experimental (optical, electronic, and thermoelectric measurements) and theoretical (band engineering/models, *ab-initio* calculations) techniques to provide these insights, and I have characterized their results in the framework of existing physical models. I have developed theoretical models, as needed, to explain the large discrepancy in the computed Goldsmid-Sharp band gap for n-type and p-type ZrNiSn compounds, and I have generalized the findings to be useful for any arbitrary electron-to-hole weighted mobility ratio ( $A$ ). Through a combination of experimental measurements and a thorough application of electron band/transport physics I provide a novel interpretation to the properties in these systems